Theoretical simulation and analysis of large size BMP-LSC by 3D Monte Carlo ray tracing model*

Feng Zhang(张峰)[1], Ning-Ning Zhang(张宁宁)[1], Yi Zhang(张义)[3], Sen Yan(闫森)[1], Song Sun(孙松)[1,2], Jun Bao(鲍骏)[1,2,†], and Chen Gao(高琛)[1,2,‡]

[1] *National Synchrotron Radiation Laboratory, Collaborative Innovation Center of Chemistry for Energy Materials, University of Science and Technology of China, Hefei* 230029, *China*

[2] *CAS Key Laboratory of Materials for Energy Conversion, Department of Materials Science and Engineering, University of Science and Technology of China, Hefei* 230026, *China*

[3] *College of Science, Sichuan Agricultural University, Ya'an* 625014, *China*

(Received 8 December 2016; revised manuscript received 4 January 2017; published online 6 April 2017)

Luminescent solar concentrators (LSC) can reduce the area of solar cells by collecting light from a large area and concentrating the captured light onto relatively small area photovoltaic (PV) cells, and thereby reducing the cost of PV electricity generation. LSCs with bottom-facing cells (BMP-LSC) can collect both direct light and indirect light, so further improving the efficiency of the PV cells. However, it is hard to analyze the effect of each parameter by experiment because there are too many parameters involved in the BMP-LSC. In this paper, all the physical processes of the light transmission and collection in the BMP-LSC were analyzed. A three-dimensional Monte Carlo ray tracing program was developed to study the transmission of photons in the LSC. A larger-size LSC was simulated, and the effects of dye concentration, the LSC thickness, the cell area, and the cell distance were systematically analyzed.

Keywords: luminescent solar concentrators (LSC), Monte Carlo ray tracing, parameter optimization, loss mechanism of photons

PACS: 42.15.Dp, 42.79.Ek, 88.40.–j, 88.40.F– **DOI:** 10.1088/1674-1056/26/5/054201

1. Introduction

Because of the increasing demand on energy, solar energy is attracting increasing attention due to its significant advantages. As one of the most important branches of the solar energy industry, photovoltaic (PV) electricity generation has developed faster and faster in recent years.[1–3] However, the efficiency of PV cells is low and the cost is high in spite of many years development. It still remains expensive relative to competing forms of energy sources.[4] In order to decrease the cost of PV electricity generation, light concentration is an important way to achieve power gain.[5–7] Under the guidance of this idea, the luminescent solar concentrator (LSC) appeared.

As early as 1976, the idea of an optical waveguide to collect sunlight was proposed by Lambe and Weber,[8] and it experienced rapid development in the following decades.[9–15] LSC is composed of PV cells and fluorescent dyes which are uniformly distributed in the waveguide that consists of transparent material, as shown in Fig. 1. Solar light shining in the LSC is absorbed and reemitted by dyes. The new photons reemitted by dyes whose emission angle is smaller than the critical angle will escape and the rest will be trapped in the waveguide through total internal reflection and be redirected to the PV cells attached to the edges of the waveguide. Unlike traditional solar concentrators, the LSC concentrates both diffuse light and direct light, which makes a sun tracking system unnecessary.[16–18] Due to the narrow absorption band of existing fluorescent materials and other reasons, the efficiency of LSC is still low.[11,19–21] In order to collect more photons, Mansour developed an LSC with bottom-facing cells (BMP-LSC) that can absorb both direct sunlight and wave-guided light,[22] which is considered as a more effective way for cost reduction.[23–26]

Researchers have paid a lot of attention to modeling LSCs.[27–33] Theoretical calculation is an important means to analyze and optimize LSCs. At present, two main kinds of theoretical models, the thermodynamic model and the light-tracing model, have been developed.[18] The thermodynamic model is based on the energy transfer between mesh points in the LSC, and the whole volume of LSC is integrated.[27] Light-tracing for LSC uses a basic light-tracing principle, which means that a photon is traced until it leaves the LSC throught escape or absorption. Whether a physical process has occurred or not is determined by comparing the probability of a single physical process with a randomly generated number. Finally, the fate of numerous photons was tallied. The Monte Carlo light-tracing model affords greater flexibility so that it is widely used in complex systems. Carrascosa *et al.* simulated monolayer and multilayer LSC films doped with

*Project supported by the National Natural Science Foundation of China (Grant No. U1632273) and the Chinese Universities Scientific Fund (Grant No. CX3430000001).

†Corresponding author. E-mail: baoj@ustc.edu.cn

‡Corresponding author. E-mail: cgao@ustc.edu.cn

© 2017 Chinese Physical Society and IOP Publishing Ltd

Rholdamine6G and Flourol555 dyes,[28] and the results agree with the experiment. Wilton *et al*. simulated the PbSe quantum dot LSC by ray tracing model.[31] Leow *et al*. simulated the fluorescence transmission process of BMP-LSC by two-dimensional light tracing model,[32] in which the effects of optical waveguide thickness, cell width and spacing on the efficiency of the LSC cell are analyzed. In short, to better optimize the LSC parameters and increase the efficiency of LSC, the simulation of the LSC is very necessary.

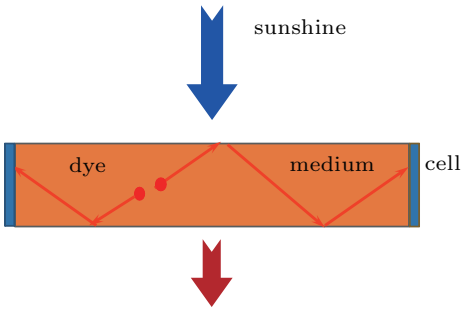


Fig. 1. (color online) The diagram of LSC.

Comparing with edge-mounted PV cell LSCs, more parameters are involved in the BMP-LSC, so optimizing the system experimentally is time consuming and difficult. Meanwhile, by the theoretical calculation, it can also be more convenient to analyze and calculate the loss mechanism of fluorescence. However, there has been less research on large size LSCs, although the large size LSC is what we will use eventually.[15,34] In this paper, a three-dimensional (3D) Monte Carlo program is written in Matlab and used to compute the performance of a large-size LSC. The contribution of each optical loss mechanism and the effects of PV cells area, PV cells position, LSC thickness, and dyes concentration were simulated.

2. Theoretical model

Seventy-two PV cells were arranged in a Tic-Tac-Toe layout as shown in Fig. 2. PMMA was chosen as the transparent material of LSC for its low cost as well as low extinction coefficient.[27,28,35] Single crystalline silicon solar cells, which have the band gap width of 1.1 eV, were attached to the bottom of the waveguide. A mass ratio of 2:1 fluorescent dyes Lumogen Red 305[10,31,34] and Yellow 083 were mixed and uniformly distributed in the optical waveguide. Figure 3 shows the emission and absorption spectrums of Red 305 and Yellow 083.

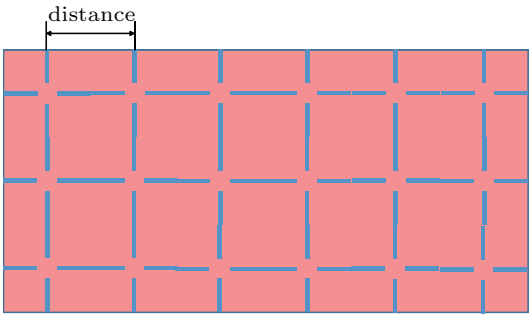


Fig. 2. (color online) The arrangement of solar cells on the LSC.

The Monte Carlo light-tracing model of LSCs was created using matlab to evaluate the device performance. A minimum of 100000 photons were created in each run. The light-tracing algorithm flow chart is depicted in Fig. 4.

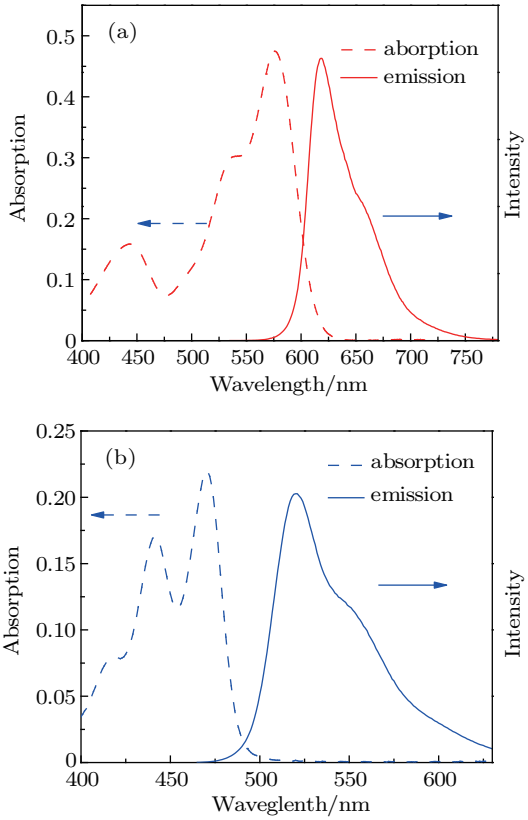


Fig. 3. (color online) The emission and absorption spectrums of (a) Red 305 and (b) Yellow 083.

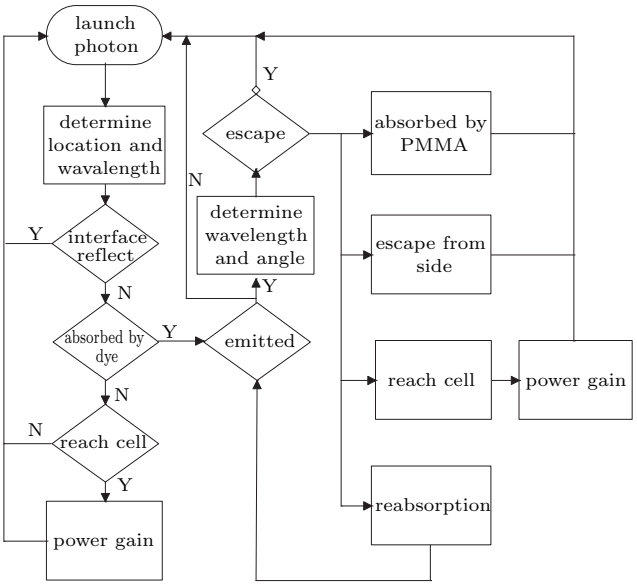


Fig. 4. Light-tracing algorithm flow chart.

AM1.5 was used as the initial emission light and only the photons which have wavelength smaller than 1124 nm will be launched. Rest photons cannot be absorbed by cells as well as dyes, so have no effect on the LSC. The photons are given a direction perpendicular to the LSC top face, and a starting position on the LSC top surface evenly over the entire panel. The probability of reflection at the LSC top face is calculated by Fresnel's equation of the incident photons at the air–PMMA interface

$$R = \left(\frac{\mathrm{n}_2 - n_1}{n_2 + n_1}\right)^2, \tag{1}$$

where $n_2 = 1.5$ represents the refractive index of PMMA and $n_1 = 1$ represents the refractive index of air. The probability of top face reflection is 0.04.

The probability of absorption and the absorption location is determined by the Beer–Lambert law

$$s = \frac{-\log_{10}(\zeta_1)}{\mu_\mathrm{r}(\lambda)C_\mathrm{r} + \mu_\mathrm{y}(\lambda)C_\mathrm{y}}, \tag{2}$$

where s represents the photons transmission distance and C is the concentration of dyes. $\mu_\mathrm{r}(\lambda)$ and $\mu_\mathrm{y}(\lambda)$, the absorption coefficients of Red 305 and Yellow 083, are measured as functions of wavelength in our laboratory with a Jobin Yvon LUOROLOG-3-TAU spectrometer. ζ_1 is a random variable that is uniformly distributed between [0, 1]. When s is the smaller than the thickness of the waveguide, it can be considered that the photon is absorbed by dyes. Otherwise, the photon is unabsorbed. The absorption spectrums of Red 305 and Yellow 083 have been given in the previous paper. Whether the surviving (not absorbed by dyes as well as PMMA) photons reach cells is determined by their position and cells. When the photons is absorbed by dyes, if

$$\zeta_2 < \frac{\mu_\mathrm{r}(\lambda)C_\mathrm{r}}{\mu_\mathrm{r}(\lambda)C_\mathrm{r} + \mu_\mathrm{y}(\lambda)C_\mathrm{y}}, \tag{3}$$

it can be considered that the photon is absorbed by Red 305. Otherwise, the photon is absorbed by Yellow 083.

When the photon is absorbed by the dyes, it is reemitted only if

$$\zeta_3 < QY, \tag{4}$$

where QY is the quantum yield of dyes and ζ_3 is a random variable. Next, the photon's new wavelength is sampled randomly from the measured emission spectrum, as if the luminescence were memoryless. The remitted direction of the photons is determined isotropically, so the azimuth (φ) is uniform from 0 to 2π, as well as the polar angle (θ) according to

$$P(\theta) = \sin\theta. \tag{5}$$

Whether the photon transfers or escapes is determined by comparing the critical angle of reflection (θ_0) and θ. The critical angle is determined by the refractive index of the transparent medium:

$$\cos\theta_0 = \sqrt{1 - \frac{1}{n_2^2}}. \tag{6}$$

If the photon's polar angle is larger than the critical angle, it will be trapped in the waveguide through total internal reflections, and then be redirected to the PV cells. Whether the photons reach the cell is determined by each point of total reflection.

When the photon is determined to have reached the cell, the path length will be calculated from the azimuth, polar angles, and total reflection times by trigonometry:

$$s_1 = t \cdot N_0/(\sin\theta \cdot \sin\varphi). \tag{7}$$

At the same time, the absorption path-length (s_2) is determined by the Beer–Lambert law at the emission wavelength

$$s_2 = \frac{-\log_{10}(\zeta_4)}{\mu_\mathrm{r}(\lambda)C_\mathrm{r} + \mu_\mathrm{y}(\lambda)C_\mathrm{y} + \alpha}, \tag{8}$$

where α is the absorption coefficient of PMMA. When s_1 is smaller than s_2, the photon is considered to have reached the solar cell. Otherwise, the photon is considered to be absorbed.

When

$$\zeta_5 < \frac{\mu_\mathrm{r}(\lambda)C_\mathrm{r}}{\mu_\mathrm{r}(\lambda)C_\mathrm{r} + \mu_\mathrm{y}(\lambda)C_\mathrm{y} + \alpha}, \tag{9}$$

the photon is considered to be absorbed by Red 305; else if

$$\zeta_5 > \frac{\mu_\mathrm{r}(\lambda)C_\mathrm{r} + \mu_\mathrm{y}(\lambda)C_\mathrm{y}}{\mu_\mathrm{r}(\lambda)C_\mathrm{r} + \mu_\mathrm{y}(\lambda)C_\mathrm{y} + \alpha}, \tag{10}$$

the photon is considered to be absorbed by Yellow 083; otherwise, the photon is considered to be absorbed by PMMA. If the photon is considered to be reabsorbed, the position can be calculated and a new photon will be emitted according to the PQ and emission spectrum.

Finally, the photons that reach the cell are tallied, and the optical efficiency is calculated by

$$\eta_\mathrm{opt} = \frac{N_\mathrm{cell}}{N_\mathrm{in}}, \tag{11}$$

where N_cell is the photons collected by cell and N_in is the total launched photons.

In the terms of practicability, the power efficiency draws more attention. The power of cells can be calculated by

$$P = I_\mathrm{SC} V_\mathrm{OC} FF, \tag{12}$$

where the fill factor FF and the open-circuit voltage V_OC are assumed to be constant. The short-circuit current I_SC is proportional to photons which reach the cells. In this model, we can get

$$I_\mathrm{SC} \propto N_\mathrm{cell}, \tag{13}$$

since N_{cell} represents the photons that reached the cells.

It can be considered that the power efficiency is proportional to optical efficiency

$$\eta_{\text{power}} = \eta_{\text{opt}}\eta_{\text{PV}}, \tag{14}$$

where η_{PV} is the photoelectric conversion efficiency of PV cells, the specific figure of which is 17% for single crystalline silicon cells.

In order to facilitate the analysis, power gain (G) was defined by

$$G = \eta_{\text{opt}}\frac{A_{\text{LSC}}}{A_{\text{PV}}}, \tag{15}$$

where A_{PV} is the total area of all the cells and A_{LSC} is the front surface area of the LSC.

3. Results and discussion

3.1. Effect of dye concentration

Dye concentration is a very important parameter in the process of solar light collection and fluorescence transmission. On one hand, high concentration of the dye can increase the absorption of the sunlight, thereby increasing the fluorescence. On the other hand, the high concentration of dye will increase reabsorption, which is expected to result in the decrease of the efficiency. Specific attention was given to simulate a rectangular LSC with dimension of 122 cm×61 cm×0.7 cm, on which 72 stripe cells with 7.8 cm×2 cm were attached and the distance between cells is 20.3 cm, as shown in Fig. 2.

As the concentration of dyes increases from 5 ppm to 160 ppm, the power gain raises steeper and then declines gently (Fig. 5(a)). The maximum gain of 1.2 appears at 80 ppm, which is equivalent to the energy efficiency of 3.2%. The fluorescence and direct light contributions to the power gain are shown in Fig. 5(b). The fluorescence contribution increases with the concentration at first and then saturates, while the direct light contribution varies in a reverse way. The direct light is the main source of the power gain, as the photons absorbed by dye are very limited although two kinds of dyes were used. It is why the bottom cell is important as it can absorb direct light. Only little photons are absorbed by Yellow 083 (1/6 of Red 305) (Fig. 5(c)), however it still contributes a little to the power gain since the absorption range of Yellow 083 is mainly at the absorption gap of Red 305. In the whole fluorescence transmission of LSC, the reabsorption is a problem that attracts a lot of attention.[19,36] It is also a very complex and complicated physical process. In order to facilitate the analysis, only the relationship between the time of iteration reabsorption and fluorescence concentration is discussed. As shown in Fig. 5(d), reabsorption increases as concentration increases. When the concentration is larger than 80 ppm, the photons absorbed by dye change slowly while the reabsorption is still increasing fast. This is mainly due to the tailing of Red 305 absorption spectrum which extends to the emission spectrum. Although the tailing part of the absorption spectrum is weak, with the increase of the dye concentration, the reabsorption capacity increases and causes strong reabsorption.

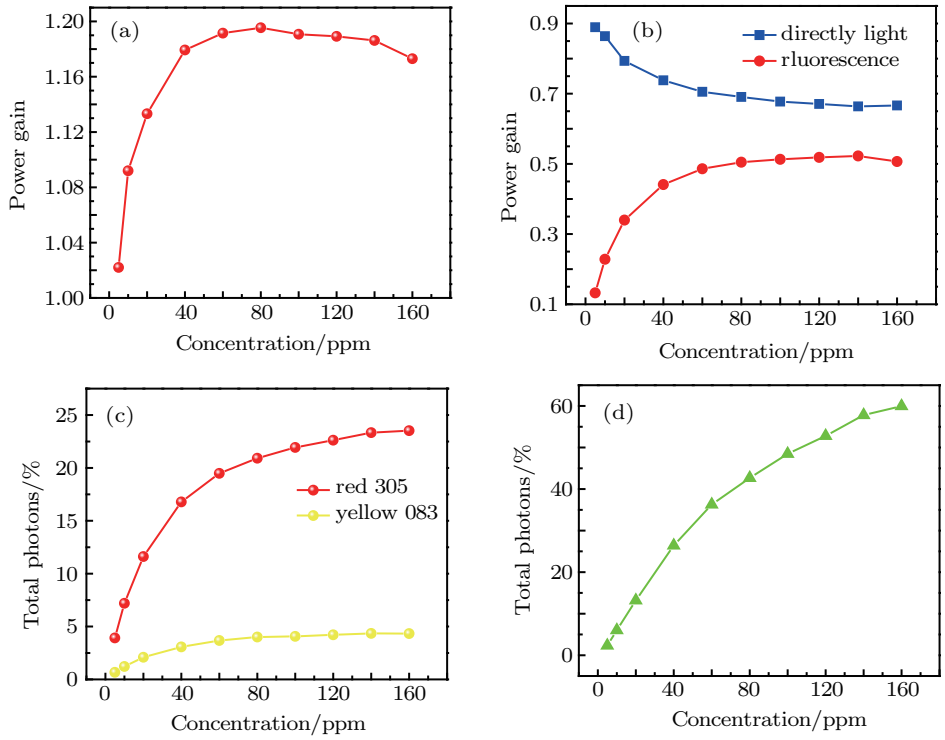


Fig. 5. (color online) (a) Power gain changes with the increase of dye concentrate. (b) The direct light and fluorescence which arrive at cells change with the increase of dye concentration. (c) The absorption of two kinds of dye. (d) The reabsorption changes with dye concentrate.

The contribution of each optical loss mechanism in LSCs can be calculated using the Monte Carlo simulation via dividing lost photons into different types based on when the loss event occurred. In principle, optical losses in a BMP-LSC can be attributed to six mechanisms: unabsorbed loss, escaping cone loss, non-radiative, interface reflection, PMMA absorption, and escape from sides. Incident photons reflecting off the top face of the LSC is always 4% and irrespective of dye concentration. The loss ratio of the other mechanisms is given in Fig. 6. Unabsorbed losses is the biggest part. This is attributed to the narrow absorption bandwidth of dyes. With the increase of concentration, more absorption, reabsorption, and thereby more reemission occurred. The latter causes more photons to leave the LSC through an escape cone. Extending Stokes shift of dyes and increasing the refractive index of the waveguide are solutions to this issue. The optical losses caused by PMMA absorption and non-radiative contribute only a small part to the total loss, which is mainly thanks to the low absorption coefficient of PMMA and high quantum efficiency of Red 305 and Yellow 083. It is worth noticing that less fluorescence escapes from the side, which indicates that the cells arrangement is reasonable.

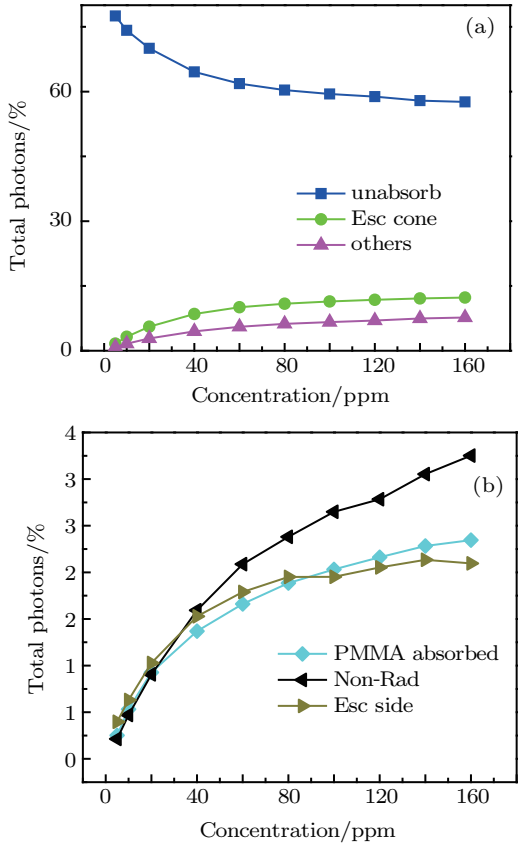


Fig. 6. (color online) Loss mechanism of LSC changes with the concentration of dyes.

3.2. Effect of LSC thickness

By increasing the thickness of LSC while keeping the total of dyes in the LSC, the concentration of dye decreases so that the reabsorption is suppressed, and the fluorescence launched by the dye does not change. The power gain under different thickness of the LSC is given in the Fig. 7.

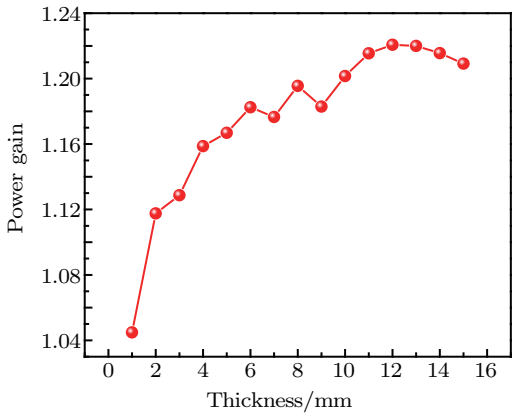


Fig. 7. (color online) Power gain changes with the thickness of LSC.

From Fig. 7, we found that the power gain increases with the increase of the thickness. However, the power gain increases slowly and eventually decreases when the thickness increases to 12 mm. In the process of fluorescence propagating along the waveguide, the probability of photon arrival to the solar cell is related with the distance of two landing positions and the width of cell. The thicker the LSC is, the larger the distance is, which leads to the increase of optical-path before reaching a cell and therefore raises the loss. The optimal thickness is 12 mm.

3.3. Effect of cell width

A simple and effective way to improve efficiency is increasing the width of the cell, which however causes the increase of cost and decrease of power gain. Shown in Fig. 8 are the power efficiency, power gain of direct light and fluorescence change as the increase of cell width.

We found that the power efficiency increases almost linearly with the width while the power gain decreases sharply as width increases. This is due to the fact that the direct light as well as the fluorescence both increase with the increase of cell width, as shown in Figs. 8(c) and 8(d). As the direct light is the main source of the output power, the power efficiency shows a nearly linear increase with the increase of cell width. Compared with direct light, the fluorescence reaching the cells changes slightly. For fluorescence, with the increase of cell width, the reabsorption is suppressed by reducing the number of reflections and the loss from side is also suppressed (Fig. 9). However, the reabsorption decreases slightly since large reabsorption occurred in a quite small optical path (Fig. 10). With increasing width, fluorescence average to a single cell area decreases, causing decrease of the power gain.

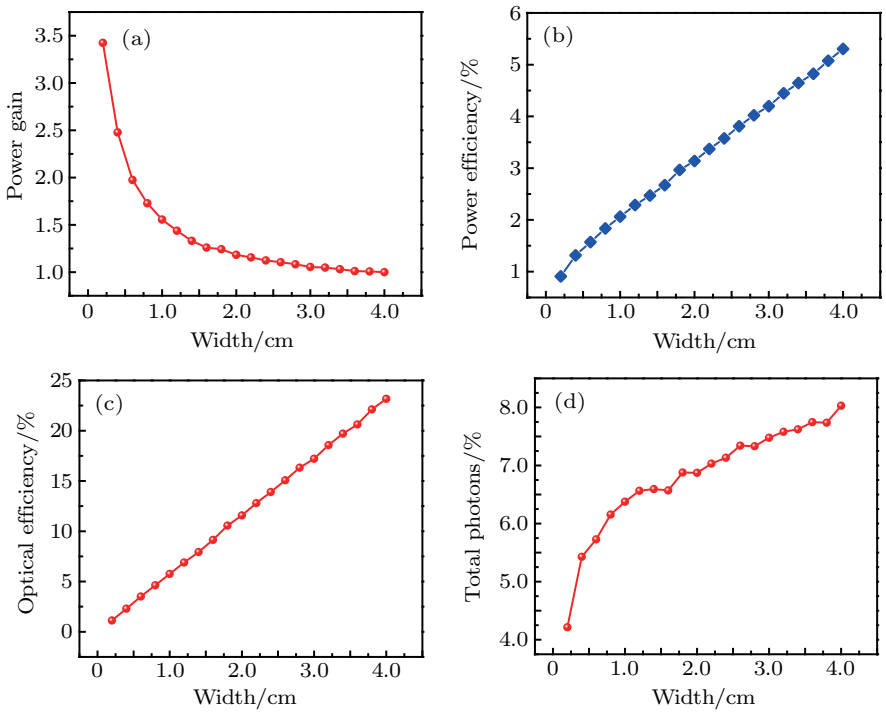


Fig. 8. (color online) (a) The power gain changes with the width of cells. (b) The power efficiency changes with the width of cells. (c) The direct light changes with the width of cells. (d) Fluorescence changes with the width of cells.

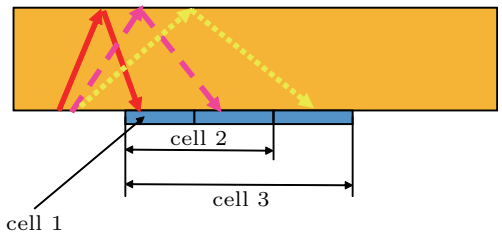


Fig. 9. (color online) Illustration of the effect of cell width on fluorescence.

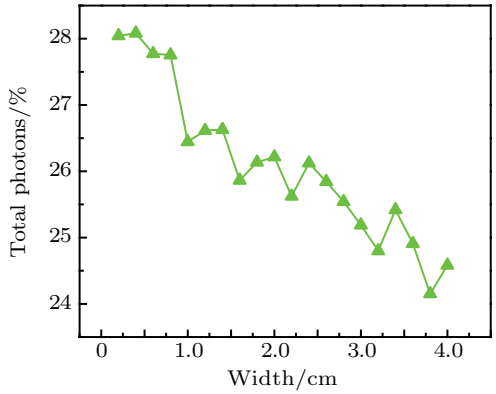


Fig. 10. (color online) The reabsorption changes with cell width.

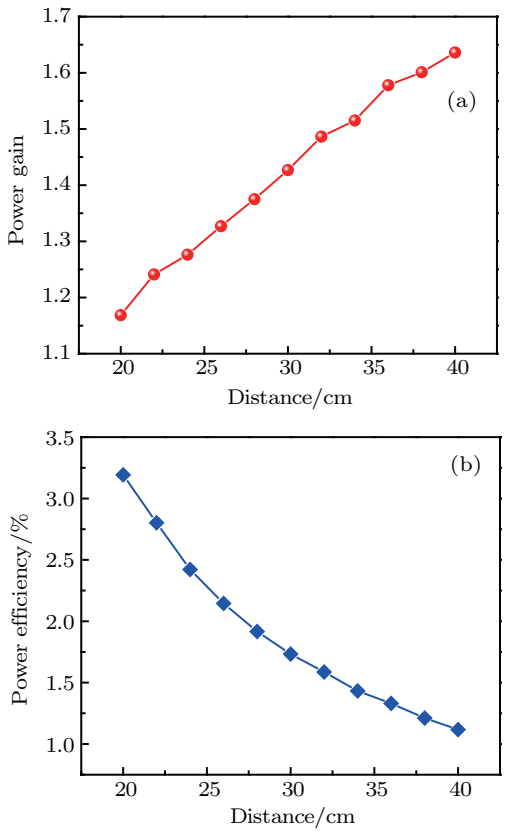


Fig. 11. (color online) (a) The power gain changes with the distance of cells. (b) The power efficiency changes with the distance of cells.

3.4. Effect of LSC size

To enhance the output power of LSC, cell distance is also a controllable parameter. A series of LSC with increasing size as well as cell distance were simulated using Monte Carlo ray tracing and the result is shown in Fig. 11.

With the size increase, the output power of LSC as well as power gain increase (Fig. 11(a)), but the power efficiency decreases rapidly (Fig. 11(b)). Larger area of LSC increases the amount of photon captured by dyes which in turn raises the

LSC output power. With the increase of LSC size and the corresponding decrease of cells coverage, the ratio of unabsorbed loss rises rapidly and thereby the power efficiency decreases. More than that, photons captured at the position further away from the PV cells experience higher probabilities of reabsorption, which is also a disadvantage.

4. Conclusion

Based on a 3D Monte Carlo model, the performance of large size BMP-LSC with Tic-Tac-Toe layout cells and two kinds of dyes was simulated. The effects of dyes concentration, wavelength thickness, cells width and distance were noted. This result can be used to guide the experiment of LSC. Moreover, by tracking the photon's travel and analyzing its final fate, a stronger understanding of the LSC physical mechanisms is obtained, which is also very helpful for further LSC design and development. Furthermore, from the simulation results, a good luminescent dye should have a narrow absorption bandwidth and big Stokes shift, which plays a crucial role on the performance of BMP-LSCs.

References

[1] Conibeer G 2007 *Mater. Today* **10** 42
[2] Zhao S Q, Zhang J R, Shi H J, Yan K K, Huang C, Yang L M, Yang R and Zhao K 2016 *Chin. Phys. B* **25** 027202
[3] Yücedağ I, Kaya A, Altındal Ş and Uslu I 2014 *Chin. Phys. B* **23** 047304
[4] van Sark W G J H M 2013 *Renew. Energ.* **49** 207
[5] Khonkar H, Alyahya A, Aljuwaied M, Halawani M, Al Saferan A, Al-Khaldi F, Alhadlaq F and Wacaser B A 2014 *Sol. Energy* **110** 268
[6] Sonneveld P J, Swinkels G L A M, van Tuijl B A J, Janssen H J J, Campen J and Bot G P A 2011 *Sol. Energy* **85** 432
[7] Su Y, Kulacki F A and Davidson J H 2014 *Sol. Energy* **107** 145
[8] Weber W H and Lambe J 1976 *Appl. Optics* **15** 2299
[9] Batchelder J S, Zewail A H and Cole T 1979 *Appl. Optics* **18** 3090
[10] Desmet L, Ras A J M, de Boer D K G and Debije M G 2012 *Opt. Lett.* **37** 3087
[11] Currie M J, Mapel J K, Heidel T D, Goffri S and Baldo M A 2008 *Science* **321** 226
[12] Shcherbatyuk G V, Inman R H, Wang C, Winston R and Ghosh S 2010 *Appl. Phys. Lett.* **96** 191901
[13] Li H, Wu K, Lim J, Song H J and Klimov V I 2016 *Nat. Energy* **1** 16157
[14] Koeppe R, Sariciftci N S and Buchtemann A 2007 *Appl. Phys. Lett.* **90** 181126
[15] Zhang J, Wang M J, Zhang Y, He H, Xie W, Yang M M, Ding J J, Bao J, Sun S and Gao C 2015 *Sol. Energy* **117** 260
[16] Debije M G and Verbunt P P C 2012 *Adv. Energy Mater.* **2** 12
[17] Rowan B C, Wilson L R and Richards B S 2008 *IEEE J. Sel. Top. Quant.* **14** 1312
[18] van Sark W G J H M, Barnham K W J, Slooff L H, Chatten A J, Buchtemann A, Meyer A, McCormack S J, Koole R, Farrell D J, Bose R, Bende E E, Burgers A R, Budel T, Quilitz J, Kennedy M, Meyer T, Donega C D M, Meijerink A and Vanmaekelbergh D 2008 *Opt. Express* **16** 21773
[19] Erickson C S, Bradshaw L R, McDowall S, Gilbertson J D, Gamelin D R and Patrick D L 2014 *ACS Nano* **8** 3461
[20] Chuang C H M, Brown P R, Bulovic V and Bawendi M G 2014 *Nat. Mater.* **13** 796
[21] Green M A, Ho-Baillie A and Snaith H J 2014 *Nat. Photonics* **8** 506
[22] Mansour A F 2003 *Polym. Test.* **22** 491
[23] Corrado C, Leow S W, Osborn M, Chan E, Balaban B and Carter S A 2013 *Sol. Energ. Mat. Sol. C.* **111** 74
[24] Zhang Y, Sun S, Kang R, Zhang J, Zhang N N, Yan W H, Xie W, Ding J J, Bao J and Gao C 2015 *Energ. Convers. Manage.* **95** 187
[25] de Boer D K G, Bruls D and Jagt H 2016 *Opt. Express* **24** A1069
[26] Vishwanathan B, Reinders A H M E, de Boer D K G, Desmet L, Ras A J M, Zahn F H and Debijed M G 2015 *Sol. Energy* **112** 120
[27] Chatten A J, Barnham K W J, Buxton B F, Ekins-Daukes N J and Malik M A 2004 *Semiconductors+* **38** 909
[28] Carrascosa M, Unamuno S and Agullolopez F 1983 *Appl. Optics* **22** 3236
[29] Krumer Z, Pera S J, van Dijk-Moes R J A, Zhao Y M, de Brouwer A F P, Groeneveld E, van Sark W G J H M, Schropp R E I and Donega C D 2013 *Sol. Energ. Mat. Sol. C.* **111** 57
[30] Sahin D, Ilan B and Kelley D F J 2011 *Appl. Phys.* **110** 033108
[31] Wilton S R, Fetterman M R, Low J J, You G J, Jiang Z Y and Xu J 2014 *Opt. Express* **22** A35
[32] Leow S W, Corrado C, Osborn M and Carter S A 2013 *Proc. SPIE* **8821** 882103
[33] Sansregret J, Drake J M, Thomas W R L and Lesiecki M L 1983 *Appl. Optics* **22** 573
[34] Meinardi F, Colombo A, Velizhanin K A, Simonutti R, Lorenzon M, Beverina L, Viswanatha R, Klimov V I and Brovelli S 2014 *Nat. Photonics* **8** 392
[35] Li X H, Fan R W, Xia Y Q, Liu W and Chen D Y 2007 *Chin. Phys.* **16** 3681
[36] Olson R W, Loring R F and Fayer M D 1981 *Appl. Optics* **20** 2934